

Optimization of RFX-mod2 gap configuration by estimating the magnetic error fields due to the passive structure currents

Lionello Marrelli^a, Giuseppe Marchiori^{a,*}, Paolo Bettini^{a,b}, Roberto Cavazzana^a, Bernard Kapidani^c, Luca Grandò^a, Nicolò Marconato^a, Ruben Specogna^c, Dimitri Voltolina^{a,b}

^a Consorzio RFX, Corso Stati Uniti 4, 35127, Padova, Italy

^b Dipartimento di Ingegneria Industriale (DII), Università di Padova, 35131, Padova, Italy

^c Dipartimento Politecnico di Ingegneria e Architettura, Università di Udine, Udine, Italy

ARTICLE INFO

Keywords:

RFP
RFX-mod
Magnetic error fields
Eddy currents
FEM code

ABSTRACT

A major refurbishment of the toroidal complex of the RFX-mod device is in progress and will include the removal of the Inconel vacuum vessel and a modification of the stainless steel supporting structure to be made vacuum tight. The plasma facing graphite tiles will be mounted onto the inner surface of the copper shell so as to increase the plasma proximity factor. New operation regimes are expected to provide a significant reduction of the amplitude of RFP tearing modes with magnetic chaos mitigation and confinement improvement. On the other hand, due to the shorter distance from the passive structures, the plasma is expected to be even more sensitive to magnetic field errors at the plasma boundary, produced by the induced currents near the cuts of the same structures. In preparation to the new RFX-mod2 experiments, a thorough revision of the conditions triggering the error fields due to the eddy currents was undertaken. An analysis of the static and dynamic equilibrium magnetic field has been carried out in RFX-mod and RFX-mod2 to estimate the magnetic field driving the shell eddy currents. A lower equilibrium magnetic field should be required in RFX-mod2. Analyses of different configurations of the poloidal gap were also carried out by a specialized computational tool. A solution with a spaced poloidal gap and a more extended overlapping was envisaged capable of maintaining the same error fields at the closer plasma boundary with the same forcing field and meeting the more stringent insulation and assembly requirements of RFX-mod2.

1. Introduction

RFX-mod [1] is undergoing a refurbishment (RFX-mod2), aimed at improving the RFP plasma boundary conditions by increasing the conductivity of the innermost structure which encloses the plasma. In detail, the RFX-mod2 design includes the removal of the Inconel vacuum vessel, the installation of the first wall graphite tiles on the inner surface of the copper shell, now to be fastened onto the stainless steel toroidal support structure (TSS), which, in turn, shall be made vacuum tight [2].

The higher conductivity of the nearest structure surrounding the plasma (copper with respect to Inconel) is expected to allow for spontaneous Tearing Modes rotation at higher plasma current [3,4] compared to RFX-mod. Moreover, the increased proximity between plasma radius and conducting shell is also expected to clamp the saturation amplitude of the tearing modes at a lower value [3]. Finally, a loop voltage reduction is also expected, due to the enlarged plasma cross

section.

On the other hand, due to the shorter distance from the shell, the plasma will be even more sensitive to magnetic field errors at its boundary, produced by the shell eddy currents near the poloidal cut (also named gap) for the penetration of the electric and magnetic fields and the holes for diagnostic access. The overlapped poloidal gap concept [1], developed for RFX-mod, represented a significant improvement in terms of error field passive reduction, compared to the RFX butt-joint. This design needs to be updated as the RFX-mod2 shell will be in vacuum, posing several additional mechanical constraints. A previous study for RFX-mod2 [5] assessed that error field reduction in a butt-joint concept with active coils would have been very challenging. In order to give the mechanical designer more freedom and to guarantee an insulation margin, a different concept, based on a separate copper toroidal section (sleeve) extending over a wide poloidal gap, has also been investigated.

The main source of shell eddy currents and associated error fields in

* Corresponding author.

E-mail address: giuseppe.marchiori@igi.cnr.it (G. Marchiori).

<https://doi.org/10.1016/j.fusengdes.2019.01.054>

Received 3 October 2018; Received in revised form 18 December 2018; Accepted 9 January 2019

Available online 12 January 2019

0920-3796/ © 2019 Elsevier B.V. All rights reserved.

the startup phase of RFX being the time variation of the net vertical field across the shell, we roughly estimate the basic static and dynamic equilibrium features of RFX-mod and RFX-mod2 (Section 2), starting from a typical RFP discharge at high current. A slightly lower vertical field will be required in RFX-mod2 due to the increased plasma minor radius [6]. The effect of different shell configurations on the field errors at plasma boundary (Section 3) are then simulated by means of CAFE [7], a specialized code that computes the induced currents in thin conducting structures with complex 3D geometry. A summary is finally given in Section 4.

2. RFX-mod and RFX-mod2: effect of the modified geometry on equilibrium and field errors

The RFX-mod plasma position is feedforward and feedback controlled [8] and a thorough experimental optimization has been performed to minimize the error fields due to the shell eddy currents. In particular, the feedforward term has been shaped to compensate for the delay in the magnetic field penetration and to oppose the Shafranov shift in an ideally conducting casing Δ_0 typically occurring in the plasma current rise phase and causing asymmetric interaction with the surrounding first wall. An assessment of the different sources of the vertical magnetic field component has been carried out for RFX-mod by processing available electromagnetic measures. Some results have been extrapolated to RFX-mod2 by running numerical models.

2.1. Experimental data analyses in RFX-mod

A procedure to estimate the currents in the Inconel vacuum vessel and in the copper shell was already validated in the past in some dedicated test vacuum pulses [9]. The reconstructed local measurements of shell surface current density and vessel filament current are taken as spatial samples of these quantities and their Discrete Fourier Transform calculated. The space distribution along the poloidal angle is then approximated by means of a finite Fourier series (up to the 3rd harmonic). The magnetic field vertical component produced by these currents can be easily computed. A typical RFP pulse at high current (shot #31895) has been considered. In Fig. 1 the average values of the vessel and shell magnetic field vertical component on a grid of points across the equatorial plane are plotted together with Shafranov plasma equilibrium field and the magnetic field vertical component produced by Field Shaping Winding (FSW) currents (the last two with the inverse sign for convenience of representation). The FSW current magnetic field is characterized by an overshoot with respect to the theoretical equilibrium field, driven by the control system feedforward signal. During the first part of the discharge, an unbalancing (outward) contribution is produced by the vessel currents because of the prevailing toroidal effect of the currents on the outer part of the vessel. This asks for an increase

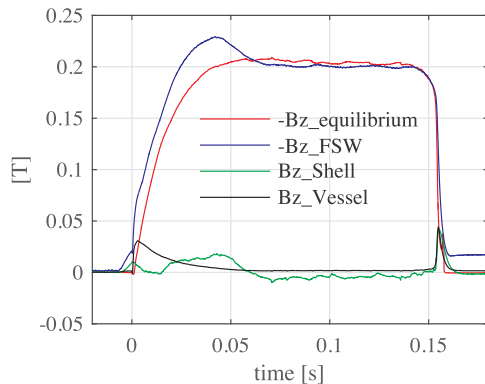


Fig. 1. Analysis of the magnetic field equilibrium vertical component in a RFP high current discharge (shot #31895).

Table 1

Plasma shift in an ideal casing (Δ_0) and compensating vertical magnetic field ($B_{z,add}$).

	RFX	RFX-mod	RFX-mod2
Δ_0 [mm]	34	14	6
$B_{z,add}$ ($\Delta = 0$) [mT]	33	17	7

in the overshoot of the FSW magnetic field to compensate for this further outward push due to the magnetic field of the vessel current. Even if the cumulative effect of plasma, vessel and FSW currents tends to maintain the shell current rather low during the very initial phase of the pulse, later on the dynamic mismatch between the applied and the required equilibrium field drives larger shell eddy currents with corresponding field errors at the cut.

2.2. A preliminary comparison between RFX-mod and RFX-mod2: static equilibrium

The static equilibrium results provided by Shafranov were applied to make a preliminary assessment of the operation of RFX-mod2, which will remain equipped with a 50 ms time constant copper shell. Shafranov plasma shift Δ_0 in an ideally conducting casing and the additional magnetic vertical field $B_{z,add}$ required for its compensation are given in Table 1 for the different versions of the RFX device. It should also be reminded that RFX-mod is operated without generating a bias vertical field in case of high current discharges so that the magnetic field $B_{z,add}$ is essentially the steady state value at the end of a transient corresponding to the plasma current rise phase. A typical value of the poloidal field asymmetry coefficient [6] $\Lambda = \beta_\theta + \frac{1}{2} - 1 \approx -0.2$ in RFX-mod RFP discharges was assumed. The smaller the shift is, the lower additional vertical field $B_{z,add}$ is required to center the plasma and the lower electric field is induced to force the eddy currents in the transient. The higher plasma proximity of RFX-mod2 should allow a further decrease in the ideal shift and the additional field. The needed total equilibrium field is slightly reduced, too.

2.3. A preliminary comparison between RFX-mod and RFX-mod2: evolutionary equilibrium and field error estimate

A further step involved an evolutionary quantitative comparison in terms of field errors between RFX-mod2 and RFX-mod. This task was performed developing an iterative procedure which exploited the approximated results provided by Shafranov equilibrium analysis [6] and the results of numerical analyses by the 3D cell method code CAFE. We started again from data of the reference shot 31895. Since the vessel will not be present in RFX-mod2, we made the further simplifying assumption to neglect it, so performing just a relative comparison between the old and new version of the device.

Thus only three field sources were considered in the procedure: the plasma current, the eddy currents induced in the 3D shell, cut along a poloidal plane, and a uniform external field source mimicking the FSW, which indeed creates a nearly uniform vertical magnetic field in the torus region. The procedure begins by computing the Shafranov approximated equilibrium poloidal flux function $\Psi_{equilibrium}(\vartheta, t)$ and splitting it into two terms, $\Psi_p(\vartheta, t)$ due to the plasma and $\Psi_{ext}(\vartheta, t)$ to all the other sources [6], i.e. the FSW currents, $\Psi_{FSW}(\vartheta, t)$, and the currents induced in the shell both by the plasma $\Psi_{eddy,p}(\vartheta, t)$ and by the FSW $\Psi_{eddy,FSW}(\vartheta, t)$. The final aim of the procedure is to determine the time evolution of the vertical field $B_{z,FSW}(t)$, produced by the FSW, that ensures equilibrium. Once the evolution of plasma current, plasma shift and poloidal asymmetry coefficient is given, the total poloidal flux function $\Psi_{equilibrium}(\vartheta, t)$ is evaluated according to Shafranov formula on a circumference of radius $r = 0.5$ m. The details of the time evolution are different for RFX-mod and RFX-mod2: in particular, the plasma shift

evolution in RFX-mod2 is obtained by rescaling the RFX-mod plasma shift evolution according to the estimated maximum value of Δ_0 (Table 1). The plasma current is modelled, in the CAFE code, by a toroidal surface current density $\mathbf{J}(\vartheta, \varphi) = \nabla\phi(\vartheta, \varphi) \times \mathbf{n}$, whose minor radius is 35 cm. The unit vector \mathbf{n} is normal to the toroidal surface and the scalar stream function is defined, as $\phi(\vartheta, \varphi, t) = \sum_{m=1,6} A_m(t)\sin(m\vartheta)$ where the time varying coefficients $A_m(t)$ are determined by a matrix inversion, in order to reproduce the time evolution of the plasma poloidal flux $\Psi_p(\vartheta, t)$. Once these terms are available, the CAFE code computes the shell eddy currents $\Psi_{eddy,p}(\vartheta, t)$. The external windings have to create a time varying vertical field $B_{z,FSW}(t)$ such that $\Psi_{FSW}(\vartheta, t) + \Psi_{eddy,FSW}(\vartheta, t) = \Psi_{ext}(\vartheta, t) - \Psi_{eddy,p}(\vartheta, t)$. The r.h.s. is known and it allows determining the l.h.s., or more precisely its cosine 1st harmonic $y_{1c}(t) = \frac{1}{\pi} \int [\Psi_{FSW}(\vartheta, t) + \Psi_{eddy,FSW}(\vartheta, t)] \cos\vartheta d\vartheta$.

The Fourier transform of the shell pulse response to an external uniform field $G(\omega)$ can be precalculated through CAFE. Then the time evolution of the uniform vertical component due to the FSW currents $B_{z,FSW}(t) = u(t)$ can be obtained by taking the inverse Fourier transform of the product $U(\omega) = G^{-1}(\omega)Y_{1c}(\omega)$, where $Y_{1c}(\omega) = F(y_{1c}(t))$ is the Fourier transform of $y_{1c}(t)$. When both the external and the internal magnetic field sources are calculated, by running CAFE again it is possible to evaluate the total shell eddy currents and their contribution to the magnetic field on the chosen surface. A dense net of virtual sensors (720 toroidal x 60 poloidal) in the numerical model allows an accurate reconstruction of the complete spatial magnetic field distribution. In the upper panel of Fig. 2 we compare the time evolutions of RFX-mod and RFX-mod2 magnetic field radial component $Br(\vartheta = 90^\circ)$ at the 3 toroidal angles indicated by the vertical lines in the lower panel (bold, thin, dashed), where the toroidal distribution of $Br(\vartheta = 90^\circ)$ is plotted at $t = 20$ ms. The two peaks correspond to the angular positions of the two shell overlapped edges. The higher peak values in RFX-mod2 in the lower panel depend on the plasma being closer to the shell overlapped edges. However, the adopted approach which leads to this worsened condition should be considered a rather conservative one. In fact, it was pointed out in Section 2.1 that the vessel currents act as a source of field opposing the equilibrium and asking for an additional amount of FSW vertical magnetic field in the plasma rise phase.

3. Alternative configurations of the shell poloidal gap in RFX-mod2

In RFX-mod2 the insertion of an insulating layer between the shell edges to avoid electric arcs at the gaps must be compatible with a reliable assembly procedure. Thus a thorough revision of the gap configuration was necessary to assess the effects on the quality of the

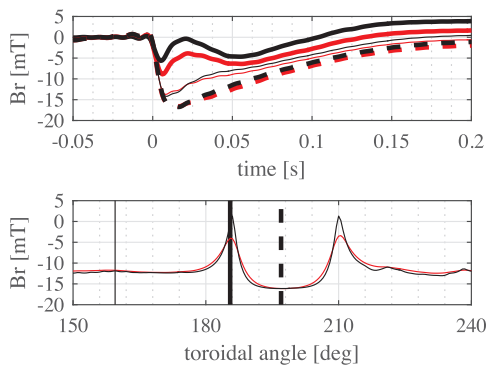


Fig. 2. Top: time evolution of $Br(\vartheta = 90^\circ)$ at three toroidal angles. Bottom: toroidal distribution of $Br(\vartheta = 90^\circ, \varphi)$ at $t = 20$ ms. RFX-mod (red) and RFX-mod2 (black) (For interpretation of the references to colour in this figure legend, the reader is referred to the web version of this article).

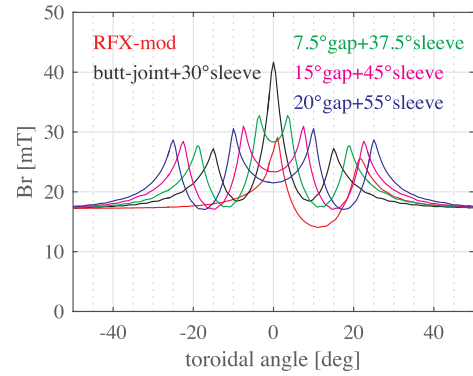


Fig. 3. Toroidal profile of $Br(\vartheta = 90^\circ, t = 50$ ms) for different gap and sleeve widths and in RFX-mod.

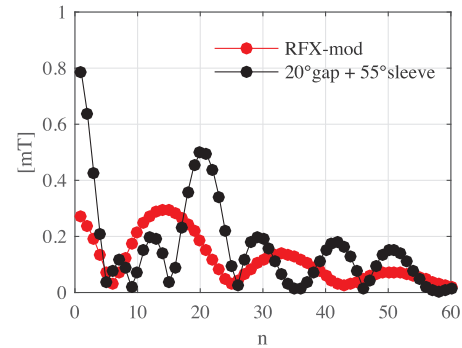


Fig. 4. Time averaged (20–50 ms) toroidal mode spectrum ($m = 1, n$) of $Br(\vartheta = 90^\circ, \varphi)$: RFX-mod (red) vs. 20° poloidal gap with 55° sleeve (black) (For interpretation of the references to colour in this figure legend, the reader is referred to the web version of this article).

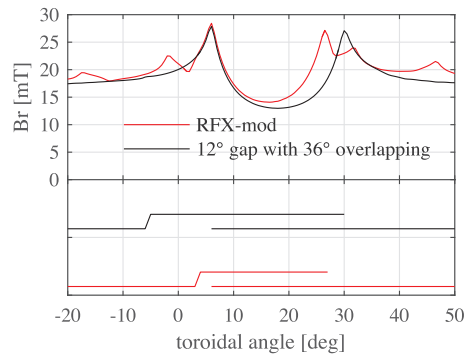


Fig. 5. Spaced poloidal gap with overlapping edges. Top: toroidal profile of $Br(\vartheta = 90^\circ, t = 50$ ms); bottom: schematic representation of the two different gap configurations.

device magnetic confinement. In the following we will focus on the more critical poloidal gap, but the optimization of the toroidal gap, which affects the $m = 0$ MHD modes, is also under way. The butt-joint gap, as in the first version of RFX, would have allowed simplifying the assembly of the toroidal complex, but previous analyses and experimental results showed that it entails unacceptable field errors [7]. The solution adopted in RFX-mod, one narrow (2 cm) gap with 22.5° overlapping, proved to be effective in reducing the field error, but it cannot be just replicated in RFX-mod2 due to both assembly and insulation requirements. This solution will be used as a benchmark to assess two alternative ones, which have been analyzed by means of the CAFE code. The previously mentioned simplified model without the support structure has been considered sufficient to perform the assessment according to a comparative approach. The results were obtained by applying a

uniform vertical forcing field with a rise time (20 ms) and an amplitude (30 m T), corresponding to the estimated dynamics of the shell eddy current driving field in RFX-mod. A Fourier analysis of the field error has also been carried out to monitor components which can trigger harmful MHD modes.

3.1. Poloidal gap with separated sleeve

The insertion of the insulation layer and the following assembly would be made easier by separating the overlapped stretch from the underlying shell. A conducting sleeve spanning a poloidal butt-joint gap could be conveniently positioned with the desired overlapping length. On the other hand, the eddy current paths at the sleeve edges and at the facing edges of the underlying butt-joint gap imply the presence of three peaks in the toroidal distribution of B_r as shown in the black curve of Fig. 3, where the distance of the parallel facing edges is 2 cm and the sleeve extension is 30°. The central peak is higher than in the original RFX-mod overlapped gap (red curve) and the amplitudes of the other two are comparable with the old one. Extension of the sleeve length (37.5°, 45° and 55°) and increased distance of the underlying shell edges (gap width: 7.5°, 15° and 20°) lead to four peaks with a trend towards an equalization of their amplitudes. The limit solution would be a gap width equal to 180° and a 220° sleeve, which is equivalent to two gaps with 20° overlapping. For the sake of clarity we restrict the comparison with RFX-mod to the best performing one. In Fig. 4 the time averaged (20–50 ms) toroidal mode spectra are shown. The difference in the two spectra depends on the enlarged extension of the magnetic perturbation in the gap region and the distances between the edges of the conducting elements. Lower n harmonics correspond to Resistive Wall Modes, that can be controlled by the RFX-mod MHD control system for both gap geometries. Higher n harmonics ($n > = 7$ for RFX-mod) have been shown to contribute to the wall-locking of the Tearing Modes [10] if their amplitude is sufficiently high: for typical RFX-mod parameters both error field spectra are not significantly affecting wall-locking.

3.2. Spaced poloidal gap with overlapped edges

The results presented in the previous section show that the electrical continuity of the overlapping stretch with one side of the shell must be retained to maintain the same error field toroidal pattern as in RFX-mod in the presence of the same forcing field. On the other hand, if the original overlapping length were kept, the need of a wider gap to guarantee a larger insulation margin would imply an increased proximity of the shell edges with a consequently higher error field peak. An improvement was achieved by extending the overlapping part by the same length as the removed underlying copper stretch. Fig. 5 shows the comparable patterns of the error field with respect to RFX-mod after

this modification. The different gap widths and overlapping lengths are schematically displayed by the lines in the bottom panel, referring to RFX-mod (red) and to the proposed solution for RFX-mod2 (black), respectively. In this case RFX-mod data were obtained by using a mesh with full details of the shell and this explains the presence of local error field peaks in the corresponding curve. It must be reminded that these peaks must be rescaled taking into account the expected favourable ratio between the forcing field in RFX-mod and RFX-mod2 suggested by the analyses of Section 2.

4. Conclusions

The design of a the new toroidal complex of RFX-mod2 with the increased proximity factor between plasma and conducting shell required a thorough investigation of the consequences in terms of quality of the magnetic field configuration at the plasma boundary. The effect of the geometric modifications from RFX-mod to RFX-mod2 on plasma equilibrium and field errors was analysed. As a result, reduced amplitude of the magnetic field forcing the circulation of the shell eddy currents was estimated for RFX-mod2. Alternative configurations of the poloidal gap were also assessed by comparing the resulting error field amplitudes and toroidal harmonic spectrum with the same forcing field. A spaced poloidal gap with a more extended overlapping seems to be the best solution to guarantee the same results in terms of error fields as in RFX-mod at the now closer plasma boundary and the capability to comply with the strict insulation and assembly requirement of RFX-mod2.

References

- [1] P. Sonato, et al., Machine modification for active MHD control in RFX, *Fusion Eng. Des.* 66 (2013) 161–168.
- [2] S. Peruzzo, et al., Design concepts of machine upgrades for the RFX-mod experiment, *Fusion Eng. Des.* 123 (2017) 59.
- [3] M. Zuin, et al., Overview of the RFX-mod fusion science activity, *Nucl. Fusion* 57 (2017) 102012.
- [4] P. Innocente, et al., Tearing modes transition from slow to fast rotation branch in the presence of magnetic feedback, *Nucl. Fusion* 54 (2014) 122001.
- [5] P. Bettini, L. Grando, G. Marchiori, Feasibility study of a local active correction system of magnetic field errors in RFX-mod, *Fusion Eng. Des.* 96–97 (2015) 649.
- [6] V.S. Mukhovatov, V.D. Shafranov, Plasma equilibrium in a tokamak, *Nucl. Fusion* 11 (1971) 605–633.
- [7] P. Bettini, et al., Modeling of the magnetic field errors of RFX-mod upgrade, *Fusion Eng. Des.* 123 (2017) 518–521.
- [8] M. Cavinato, G. Marchiori, *Fusion Eng. Des.* 74 (2005) 567–572.
- [9] G. Marchiori, L. Grando, M. Cavinato, Characterization of RFX-mod passive conducting structures to optimize plasma start up and equilibrium control, *Fusion Eng. Des.* 82 (2007) 1131–1137.
- [10] A.K. Hansen, et al., Locking of multiple resonant mode structures in the reversed-field pinch, *Phys. Plasmas* 5 (1998) 2942.